TESS observations of the interesting pulsating subdwarf B star CDS-28 1974

M. D. Reed[1⋆], K. A. Shoaf[1], M. Uzundag[2], J. Vos[3], P. Németh[3], A. S. Baran[5], R. H. Østensen[1], C. S, Jeffery[6],J. H. Telting[7], others

[1] *Department of Physics, Astronomy and Materials Science, Missouri State University, 901 S. National, Springfield, MO 65897, USA*
[2] *Instituto de Física y Astronomía y Centro de Astrofísica de Valparaíso, Chile*
[3] *Somewhere in Germany*
[4] *Astroserver.org, 8533 Malomsok, Hungary*
[5] *Suhora Observatory and Krakow Pedagogical University, ul. Podchorąży ch 2,30-084 Kraków, Poland*
[6] *Armagh Observatory and Planetarium, College Hill, Armagh BT61 9DG, UK*
[7] *,Nordic Optical Telescope, Rambla José Ana Fernández Pérez 7, 38711 Breña Baja, Spain*

Accepted Received

ABSTRACT

From TESS Sector 5 observations we have discovered CDS-28 1974 to be a pulsating subdwarf B (sdBV) star which has an unusual gravity(g)-mode asymptotic sequence. We securely detect 13 periodicities, mostly between 300 and 600μHz, which form an $\ell = 1$ asymptotic sequence near the typical period spacing. The peculiarity is that typical $\ell = 1$ g modes occur between $100 - 300\mu$Hz, while these are between $300 - 600\mu$Hz. This indicates that CDS-28 1974's structure is somewhat different from typical sdBV stars.

CDS-28 1974 has a close companion 1.113" away, which may be a physical companion. We analyze spectra we have obtained to determine whether or not this is a physical pair and what that might mean for the sdB star's evolution.

Key words:
Stars: oscillations – Stars: subdwarfs

1 INTRODUCTION

The Transiting Exoplanet Survey Satellite (TESS Ricker et al. 2016) is a set of four 100 mm aperture cameras aboard a spacecraft with a highly-eccentric, lunar-resonance Earth orbit. The orbit requires the telescope to change pointing roughly every lunar month. TESS's main mission is to detect exoplanets via the transit method (Ricker 2015), but as it is staring at stars for a month at a time, its secondary mission is asteroseismology. In that regard, continuous, two minute cadence, single-instrument observations cannot be matched by ground-based observatories. This makes TESS an excellent instrument for asteroseismology.

Asteroseismology uses stellar pulsations, which TESS views as periodic light variations, to discern stellar structure and evolution. Observationally, the goal is to associate periodicities with pulsation *modes* which are described by quantized spherical harmonics as n, ℓ, and m modes. In this case n represents the number of radial nodes, ℓ the number of nodes along the surface, and m the number of azimuthal surface modes (Aerts et al. 2010).

In this paper we analyze data for a pulsating subdwarf B (sdBV) star. Subdwarf B stars are extreme horizontal branch stars of roughly half a solar mass and 20% the radius of our Sun (for a review of sdB stars, see Heber 2016). The Kepler mission provided transformative data for sdBV stars, in that prior to Kepler data, it was rare to have observationally constrained mode identifications, but from Kepler data, identifications are routinely determined (Baran et al. 2012; Reed et al. 2011; Telting et al. 2014, e.g.). The main methods to observationally associate periodicities with modes are frequency multiplets, where azimuthal degeneracy is lifted, typically by rotation (Baran et al. 2012, e.g.), and g-mode asymptotic period sequences, where g (gravity) mode overtones (relative n) are evenly spaced in period for each degree, ℓ (see Reed et al. 2018, for a review).

We examine TESS data on the sdB star CDS-28 1974 (with TESS Identification Catalogue number (TIC) 13145616 and also HE 0505-2806). CDS-28 1974 is involved in a complex system of nearby stars, one of which may be a physical companion. Previous spectroscopic observations of CDS-28 1974 have identified it as a spectroscopic

⋆ E-mail:MikeReed@MissouriState.edu

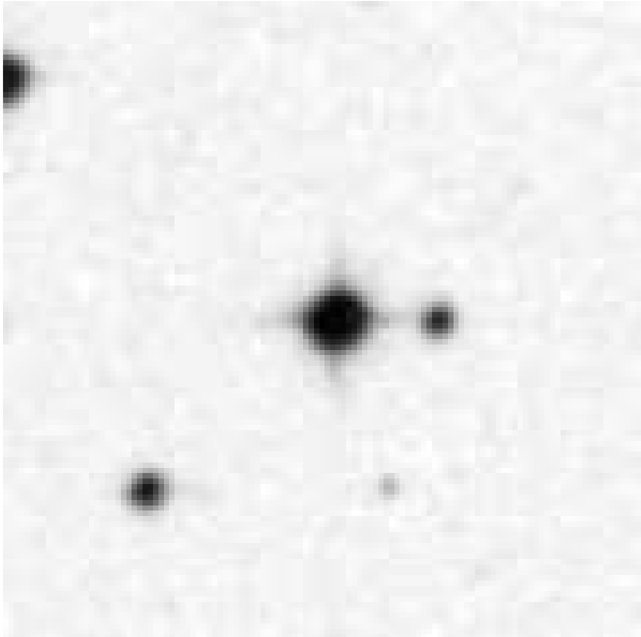

Figure 1. Digitized Sky Survey image of the CDS-28 1974 field, 2' on a side.

binary with an F or G-type companion (Vennes et al. 2011). Low-dispersion spectra obtained and fitted by Vennes et al. (2011) determined $T_{\rm eff} = 25\,000 \pm 2\,500$, $\log g = 4.90 \pm 0.35$, and $\log n({\rm HE})/n({\rm H}) = -2.2 \pm 0.5$. Németh et al. (2012) obtained three low-resolution spectra, from which they found "Changing composite features". From their individual spectra they produced wildly differing results from $T_{\rm eff} = 25\,710^{+3450}_{-1450}$, $\log g = 5.28^{+0.40}_{-0.26}$ to $T_{\rm eff} = 29\,840^{+180}_{-200}$, $\log g = 5.61^{+0.03}_{-0.06}$. Németh et al. (2012) write "An inspection of their fields revealed crowding; both stars are visual binaries. The composite spectra are most probably the result of contamination from the nearby, but possibly independent, star." Upon further inspection, it was determined that spectral decomposition could not produce realistic luminosity ratios, meaning they are not likely a physical pair. Outside of the unresolved pair, there is another star 15" away. In Fig. 1 we show a 2' square Digitized Sky Survey image. CDS-28 1974's binary status will be discussed in §3.

2 ANALYSES OF TESS DATA

CDS-28 1974 was observed as one of our Guest Investigator program (G011177) targets, as well as a TESS Asteroseismic Science Consortium (TASC) target and we downloaded the processed lightcurve from the Mikulski Archive for Space Telescopes as a GI bulk download. CDS-28 1974 was observed during S5 which spanned about 26 days from 15 November, 2018 to 11 December, 2018 and from which we used 17 421 two-minute-cadence data points after sigma clipping. Our final data set was spline fitted to remove trends > 1.5 d, though we also examined a non-fitted set to search for a binary signal. As TESS has 21" pixels, there will certainly be contamination from the nearby star, in addition to the companion. This will reduce pulsation amplitudes as we normalize them as $\Delta I / < I >$ where $< I >$ is the average intensity. We do not attempt any flux corrections as absolute amplitudes are not important to our analyses and we report amplitudes in parts-per-thousand (ppt). The data have a temperoral resolution of $1.5/T = 0.68\mu$Hz and we used a 4σ detection limit, calculated in pulsation-free regions of 55-115, 320-375, and 605-720μHz and linearly interpolated between.

The processed lightcurve was Fourier transformed (FT; top panel of Fig. 2) and subsequently converted to period (PT; bottom panel of Fig. 2) to highlight asymptotic sequences. We non-linear least-squares (NLLS) fitted the lightcurve using frequencies and amplitudes from the FT as initial estimates. The fits were then removed (prewhitened) from the lightcurve and reviewed by-eye as a measure of goodness-of-fit. The prewhitened FT is shown in the middle panel of Fig. 2. We prewhitened 13 periodicities above the 4σ detection limit and four further frequencies below it (discussed below). We note that while $f1$ has an NLLS-fitted amplitude below 4σ, the original amplitude was over the detection threshold, and therefore we consider it intrinsic to CDS-28 1974. The resultant frequencies (periods), amplitudes, and signal-to-noise (S/N) are provided in Table 1.

As discovered by Reed et al. (2011) using Kepler data, nearly all g-mode sdBV stars have asymptotic period sequences with $\ell = 1$ spacings near 250 s. As is typical, we used a Kolmogorov-Smirnov (KS) test to search for the period spacing. The results are shown in the left panel of Fig. 3. We then folded the periods over that spacing into an échelle diagram (right panel of Fig. 3) and also used a linear regression to fit the periods. The resultant period spacing is $268.85 \pm 0.32\,s$. As can be seen in the échelle diagram, there is a slight "hook" in the lower portion of the sequence, which is a feature seen in other sdBV stars (Baran & Winans 2012). From this sequence we were able to identify eight significant frequencies as $\ell = 1$ and another two as $\ell = 2$ from the relationship $\Pi_{\ell=2} = \Pi_{\ell=1}/\sqrt{3}$.

We noticed several peaks which appeared just under the detection threshold. We tested if their periods fit into the asymptotic sequences (to within 10%), and if they did, we attempted NLLS fitting and prewhitening. If that succeeded, we list them in Table 1 as *suggested* periodicities. These suggested frequencies were not used in the asymptotic sequence fit. We note that $s1$ is possibly below the acoustic cut-off, but see no harm in listing it, as it was not used to determine the asymptotic sequence. (It also is not shown in Fig. 3.)

We also searched for frequency multiplets to indicate rotation, but found none. This is not surprising as the TESS sector campaigns, while wonderful compared to what can be obtained from the ground, are mostly too short compared with known sdB rotation periods of tens of days (Reed et al. 2018).

3 DISCUSSION

From single-sector TESS data, we discovered CDS-28 1974 to be a new sdBV and detect 16 periodicities. The feature which makes CDS-28 1974 so interesting is the frequency range in which the dominant periodicities lie. Five of the six highest-amplitude periodicities occur between 400 and 600μHz. We have seen pulsations in this range before, but typically they are not the dominant amplitudes and usu-

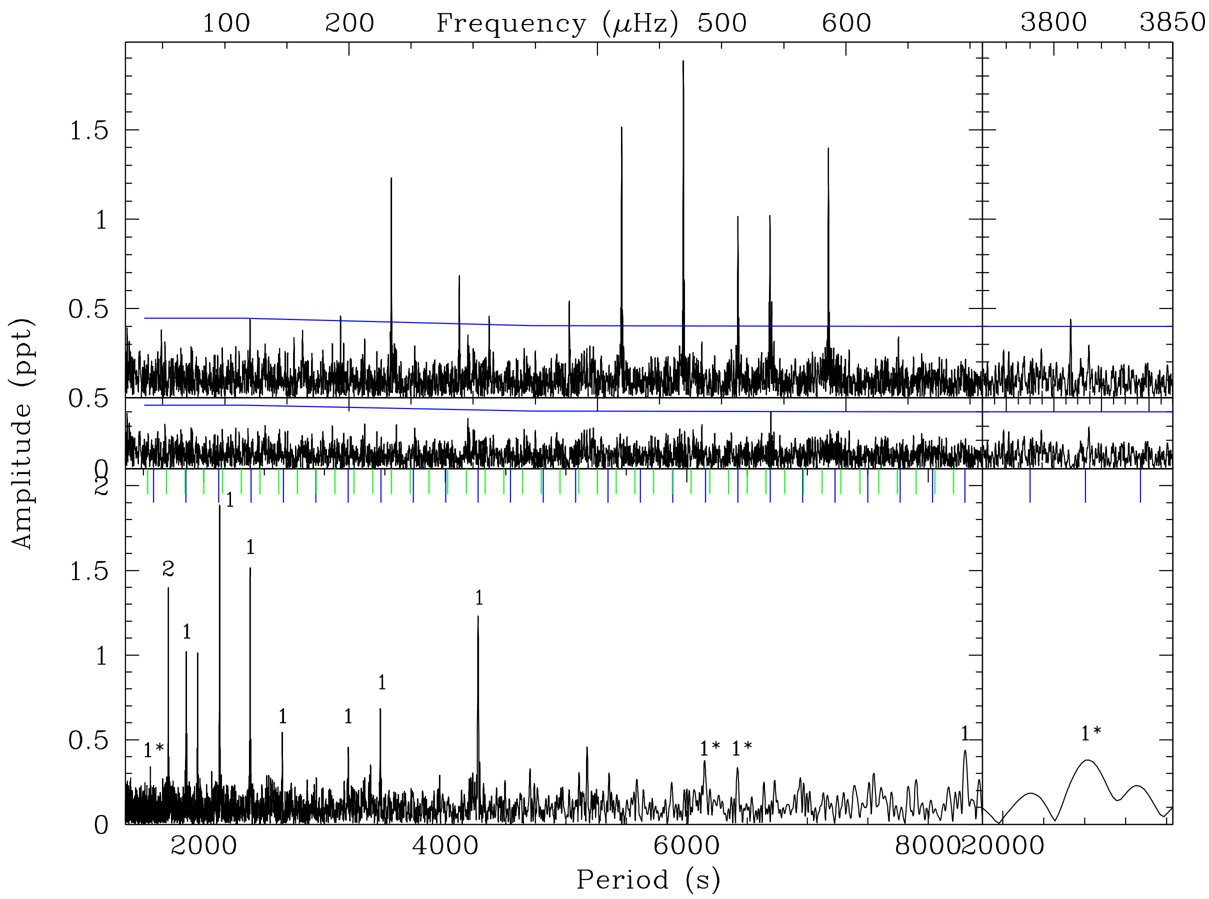

Figure 2. Fourier transform (top) and prewhitened FT (middle) including the detection limit as a horizontal line. The bottom panel shows the period transform. Labels identify the pulsations and the asymptotic sequences are indicated by lines (blue for $\ell = 1$ and green for $\ell = 2$) along the top.

Table 1. Radial indices with a † are $\ell = 2$ while the rest are identified as $\ell = 1$ modes. Periodicities identified with an "s" are below the detection threshold and are therefore *suggested* frequencies. Column 6 lists the relative radial order n and Column 7 lists the fractional deviation from the asymptotic sequence.

ID	Freq (μHz)	Period (s)	Amp (ppt)	S/N	n	DP/P (%)
s1	48.981 (55)	20416.25 (22.97)	0.385 (88)	3.35	75	4.8
f1	120.383 (48)	8306.83 (3.34)	0.438 (88)	3.81	30	0.6
s2	155.753 (64)	6420.43 (2.65)	0.330 (88)	3.01	23	-1.1
s3	162.627 (56)	6149.03 (2.13)	0.377 (88)	3.44	22	-2.0
f2	193.240 (46)	5174.91 (1.24)	0.460 (88)	4.26	–	–
f3	234.083 (17)	4271.98 (0.31)	1.232 (88)	11.65	15	-0.2
f4	288.818 (31)	3462.38 (0.37)	0.685 (88)	6.60	12	-1.4
f5	312.830 (46)	3196.63 (0.47)	0.466 (88)	4.61	11	-0.2
f6	377.377 (41)	2649.87 (0.29)	0.542 (91)	5.37	9	-3.6
f7	419.559 (14)	2383.45 (0.08)	1.521 (91)	15.03	8	-2.7
f8	469.215 (12)	2131.22 (0.05)	1.894 (91)	18.84	7	3.5
f9	513.128 (22)	1948.83 (0.08)	1.019 (91)	10.19	–	–
f10	538.930 (23)	1855.53 (0.08)	0.994 (92)	9.94	6	1.0
f11	540.361 (49)	1850.62 (0.17)	0.461 (92)	4.61	$11^{\dagger}$	3.0
f12	585.958 (16)	1706.61 (0.05)	1.401 (91)	14.06	$10^{\dagger}$	10.3
s4	642.381 (65)	1556.71 (0.16)	0.341 (91)	3.42	5	-10.2
f13	3807.044 (48)	262.67 (4)	0.438 (87)	4.39	–	–

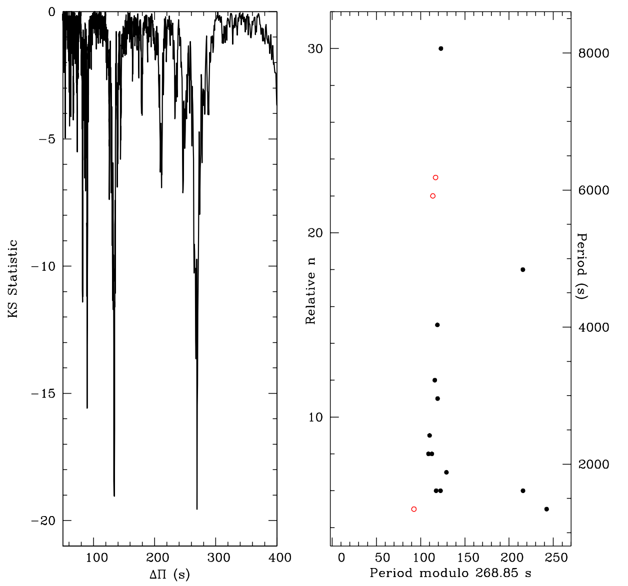

Figure 3. KS test (left) and échelle diagram (right) indicating the dominant $\ell = 1$ asymptotic sequence. (The right panel does not show $s1$ as it would compress most of the periods to the bottom.)

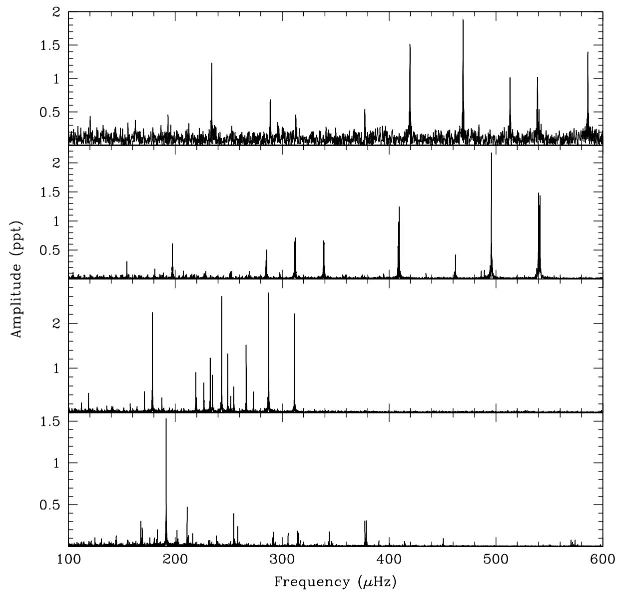

Figure 4. Comparison of FTs between the extreme outliers of Fig. 5 (Top panel is CDS-28 1974 with EQ Psc immediately below it) and "typical" g-mode sdBV stars (Bottom panel is PG 0101 and above it is HZ Cnc). Bottom three panels were observed during K2.

ally high-degree $\ell > 2$ (e.g. Foster et al. 2015; Telting et al. 2014) modes. That they are $\ell = 1$ modes is unusual. The same applies to the sdBV star EQ Psc (Baran et al. 2019), which has a slightly higher frequency for the dominant amplitude. The high-frequency pulsations in EQ Psc are also associated with $\ell = 1$ modes. These are shown in the top two panels of Fig. 4 and then compared with *typical* pulsators in the bottom two panels.

If we compare the highest-amplitude frequency with $T_{\rm eff}$, as in Fig. 5, we see that CDS-28 1974 and EQ Psc are outliers, well-separated from the other g-mode sdBV stars. We can also see in Fig. 5 that the *typical* stars form a sequence with temperature. (This will be described further in a forthcoming publication by Reed et al. 2019). As expected, the hotter stars have the higher frequencies (shorter periods). EQ Psc is known to have an M-dwarf companion while CDS-28 1974 likely has an F or G-type companion, which may not be a physical pair. However, other sdBV stars are also in binaries (indicated by the point types in the Fig. 5) and they still reside in the sequence. So binarity, in itself, seems unlikely as the cause for their deviation. It is possible that this is an indicator that their core masses differ from the so-called canonical mass of $0.47 M_{\odot}$. It has been proposed that the sdB mass distribution is related to the formation mechanism responsible for stripping off the H-rich envelope (Han et al. 2002, 2003) and so this could be an indicator of evolutionary path. Baran et al. (2019) determined a mass for EQ Psc of 0.38 ± 0.05, though they argue that their errors are most likely unrealistically small (particularly for $\log g$) and favor a canonical value. We have not attempted a mass determination for CDS-28 1974 as the nearby star will complicate any GAIA (Evans et al. 2018) distance determination (Bailer-Jones et al. 2018) and the discrepancies in the spectroscopic quantities will produce unusably large errorbars.

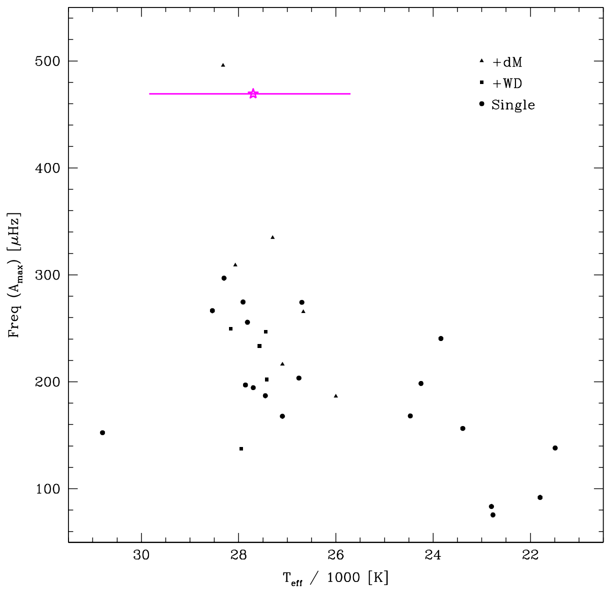

Figure 5. Comparison of effective temperature with frequency of highest amplitude periodicity. Adapted from Reed et al. (2019, in preparation) to cover only g-mode pulsators. CDS-28 1974 is the magenta star with the horizontal line indicating the range of $T_{\rm eff}$ from Németh et al. (2012).

However, the pulsations of EQ Psc and CDS-28 1974 imply there is something atypical about their structure. Here we simply report the anomaly and look forward to modelling results for an explanation.

We examined the uncorrected lightcurve of CDS-28 1974 to search for signs of binarity. This could be either ellipsoidal variations or a reflection effect. Neither effect was observed. This is not surprising even if the unresolved pair is a physical binary. To our knowledge, there are no known cases of sdB stars in short-period binaries with F or G stars. Such orbits only appear to be long, with periods of > 100 d (Vos et al. 2013, 2018). **Joris to expand this portion. The following text is merely a placeholder for his more complete solution** We have obtained five high-resolution UVES spectra at the VLT, from which we derive the usual spectroscopic quantities ($T_{\rm eff}$ and $\log g$) as well as radial velocities (RVs) and a spectral energy distribution (SED) decomposition. **UVES procedure and details here, as well as our determined values for Teff and logg**. The RVs show no significant binary motion to $\sim$ 2km·s^{-1}. There are also GAIA DR2 data (Lindegren et al. 2018), which resolves the binary into two components separated by 1.33". The two components have equal parallax and very similar proper motion, so they could be a physical pair. At the parallactic distance near 400 pc, the 1.33" separation is about 490 AU. For an sdB+F/G binary, this would be an orbital period near 9000 yr. That separation has interesting implications, should CDS-28 1974 prove to be a physical pair. That is too far apart for the F/G companion to influence the envelope-stripping mechanism to produce the sdB star. As such, there likely is, or was, an inner binary which produced the sdB star via common-envelope ejection or a merger. Considering CDS-28 1974's unusual $\ell = 1$ frequency range, this binary may warrant further investigate to determine binarity and component masses.

CDS-28 1974 has turned out to be an interesting, though not quite unique sdBV star, whose analysis was made possible by space-based continuous observations over an extended time period. We anticipate other interesting surprises as TESS will observe nearly the entire sky, including several hundred sdB stars.

ACKNOWLEDGMENTS: KAS was funded by the Missouri Space Grant, which is funded by NASA.

The Digitized Sky Surveys were produced at the Space Telescope Science Institute under U.S. Government grant NAG W-2166. The images of these surveys are based on photographic data obtained using the Oschin Schmidt Telescope on Palomar Mountain and the UK Schmidt Telescope. The plates were processed into the present compressed digital form with the permission of these institutions.

The National Geographic Society - Palomar Observatory Sky Atlas (POSS-I) was made by the California Institute of Technology with grants from the National Geographic Society.

The Second Palomar Observatory Sky Survey (POSS-II) was made by the California Institute of Technology with funds from the National Science Foundation, the National Geographic Society, the Sloan Foundation, the Samuel Oschin Foundation, and the Eastman Kodak Corporation.

The Oschin Schmidt Telescope is operated by the California Institute of Technology and Palomar Observatory.

The UK Schmidt Telescope was operated by the Royal Observatory Edinburgh, with funding from the UK Science and Engineering Research Council (later the UK Particle Physics and Astronomy Research Council), until 1988 June, and thereafter by the Anglo-Australian Observatory. The blue plates of the southern Sky Atlas and its Equatorial Extension (together known as the SERC-J), as well as the Equatorial Red (ER), and the Second Epoch [red] Survey (SES) were all taken with the UK Schmidt.

All data are subject to the copyright given in the copyright summary. Copyright information specific to individual plates is provided in the downloaded FITS headers.

Supplemental funding for sky-survey work at the ST ScI is provided by the European Southern Observatory.

REFERENCES

Aerts C., Christensen-Dalsgaard J., Kurtz D. W., 2010, Asteroseismology. Springer

Bailer-Jones C. A. L., Rybizki J., Fouesneau M., Mantelet G., Andrae R., 2018, AJ, 156, 58

Baran A. S., Reed M. D., Stello D., Østensen R. H., Telting J. H., Pakštienė E., O'Toole S. J., Silvotti R., Degroote P., Bloemen S., Hu H., Van Grootel V., Clarke B. D., Van Cleve J., Thompson S. E., Kawaler S. D., 2012, MNRAS, 424, 2686

Baran A. S., Telting J. H., Jeffery C. S., Østensen R. H., Vos J., Reed M. D., VÅÂ■cković M., 2019, MNRAS, 489, 1556

Baran A. S., Winans A., 2012, ActaAstron, 62, 343

Evans D. W., Riello M., De Angeli F., Carrasco J. M., Montegriffo P., Fabricius C., Jordi C., Palaversa L., Diener C., Busso G., Cacciari C., van Leeuwen F., 2018, ArXiv e-prints

Foster H. M., Reed M. D., Telting J. H., Østensen R. H., Baran A. S., 2015, ApJ, 805, 94

Han Z., Podsiadlowski P., Maxted P. F. L., Marsh T. R., 2003, MNRAS, 341, 669

Han Z., Podsiadlowski P., Maxted P. F. L., Marsh T. R., Ivanova N., 2002, MNRAS, 336, 449

Heber U., 2016, PASP, 128, 082001

Lindegren L., Hernandez J., Bombrun A., Klioner S., et al. 2018, ArXiv e-prints

Németh P., Kawka A., Vennes S., 2012, MNRAS, 427, 2180

Reed M. D., Baran A. S., Quint A. C., Kawaler S. D., O'Toole S. J., Telting J., et al. 2011, MNRAS, 414, 2885

Reed M. D., Baran A. S., Telting J. H., Østensen R. H., Jeffery C. S., Kern J. W., Ketzer L., Crooke J., Slayton A., 2018, Open Astronomy, 27, 157

Ricker G. R., 2015, in AAS/Division for Extreme Solar Systems Abstracts Vol. 47, The Transiting Exoplanet Survey Satellite (TESS): Discovering New Earths and Super-Earths in the Solar Neighborhood. p. 503.01

Ricker G. R., Vanderspek R., Winn J., et al. 2016, in Proc. SPIEVol. 9904 of Society of Photo-Optical Instrumentation Engineers (SPIE) Conference Series, The Transiting Exoplanet Survey Satellite. p. 99042B

Telting J. H., Baran A. S., Nemeth P., Østensen R. H., Kupfer T., Macfarlane S., Heber U., Aerts C., Geier S., 2014, A&A, 570, A129

Vennes S., Kawka A., Németh P., 2011, MNRAS, 410, 2095

Vos J., Østensen R. H., Németh P., Green E. M., Heber U., Van Winckel H., 2013, A&A, 559, A54, Paper II

Vos J., Østensen R. H., Vuckovic M., Telting J. H., 2018, A&A, p. in press